Reprinted from THE JOURNAL of the Acoustical Society of America

Vol. 87, No. 4, April 1990

Offnormal incidence reflection-coefficient determination for thick underwater acoustic panels using a generalized ONION method

Jean C. Piquette
Naval Research Laboratory, Underwater Sound Reference Detachment, P.O. Box 568337, Orlando, Florida 32856-8337

pp. 1416-1427

REPORT DOCUMENTATION PAGE

Form Approved
OMB No. 0704-0188

1. AGENCY USE ONLY (Leave blank)	2. REPORT DATE	3. REPORT TYPE AND DATES COVERED

4. TITLE AND SUBTITLE
Offnormal Incidence Reflection-coefficient Determination for Thick Underwater Acoustic Panels Using a Generalized ONION Method

5. FUNDING NUMBERS
WU = DN220-161
PE = 61153N
TA = RR011-08-42

6. AUTHOR(S)
Jean C. Piquette

7. PERFORMING ORGANIZATION NAME(S) AND ADDRESS(ES)
Naval Research Laboratory
Underwater Sound Reference Detachment
P.O. Box 568337
Orlando, FL 32856-8337

8. PERFORMING ORGANIZATION REPORT NUMBER

9. SPONSORING/MONITORING AGENCY NAME(S) AND ADDRESS(ES)

10. SPONSORING/MONITORING AGENCY REPORT NUMBER

11. SUPPLEMENTARY NOTES
Published in J. Acoust. Soc. Amer., Vol. 87, No. 4, April 1990 pp. 1416-1427.

12a. DISTRIBUTION/AVAILABILITY STATEMENT
Distribution unlimited; approved for public release.

12b. DISTRIBUTION CODE

13. ABSTRACT (Maximum 200 words)

The ONION method is a reflection-coefficient measurement technique designed for use on data acquired from thick underwater acoustic panels in the frequency range 1-10 kHz, but may be used to frequencies as high as 25 kHz. The method extrapolates transient reflected-wave data using least-squares fitting to a multiple-layer panel model. A description of the method, as it applies to data acquired using a normally incident interrogating wave, is provided in J.C. Piquette, "The ONION method: A reflection coefficient measurement technique for thick underwater acoustic panels," J. Acoust. Soc. Am. 85, 1029-1040 (1989). The present article describes research directed toward generalizing the method to allow for an offnormal incidence interrogating wave. Successful applications of the generalized method to data acquired under offnormal incidence are described. The generalized method was applied to measurements that were made on two different sample panels. The measurements involved one test temperature, two hydrostatic test pressures, and three test frequencies.

14. SUBJECT TERMS
Panel measurements, Signal extropolation,
Reflection measurements
Least squares fitting

15. NUMBER OF PAGES
12

16. PRICE CODE

17. SECURITY CLASSIFICATION OF REPORT	18. SECURITY CLASSIFICATION OF THIS PAGE	19. SECURITY CLASSIFICATION OF ABSTRACT	20. LIMITATION OF ABSTRACT
UNCL	UNCL	UNCL	UL

Offnormal incidence reflection-coefficient determination for thick underwater acoustic panels using a generalized ONION method

Jean C. Piquette
Naval Research Laboratory, Underwater Sound Reference Detachment, P.O. Box 568337, Orlando, Florida 32856-8337

(Received 15 June 1989; accepted for publication 27 November 1989)

The ONION method is a reflection-coefficient measurement technique designed for use on data acquired from thick underwater acoustic panels in the frequency range 1–10 kHz, but may be used to frequencies as high as 25 kHz. The method extrapolates transient reflected-wave data using least-squares fitting to a multiple-layer panel model. A description of the method, as it applies to data acquired using a normally incident interrogating wave, is provided in J. C. Piquette, "The ONION method: A reflection coefficient measurement technique for thick underwater acoustic panels," J. Acoust. Soc. Am. **85**, 1029–1040 (1989). The present article describes research directed toward generalizing the method to allow for an offnormal incidence interrogating wave. Successful applications of the generalized method to data acquired under offnormal incidence are described. The generalized method was applied to measurements that were made on two different sample panels. The measurements involved one test temperature, two hydrostatic test pressures, and three test frequencies.

PACS numbers: 43.20.Fn, 43.20.Px, 43.30.Sf, 43.60.Gk

INTRODUCTION

Panel measurements are a standard technique whereby the effectiveness of a coating material at reducing unwanted echoes is determined. The conventional panel-measurement method[1,2] involves the use of a sample panel whose lateral dimensions are large compared to a wavelength of the interrogating wave in the surrounding fluid medium. However, due to the difficulty and cost of fabricating large samples, and due to the limited size of test facilities, available samples often have lateral dimensions that are less than one such wavelength for frequency ranges of interest.

In order to avoid the interfering influence of the diffracted waves originating at the sample edges, it is often necessary to operate a panel test in the pulsed mode, and to utilize portions of the experimentally measured reflected-wave pulses that have not achieved steady state. One technique for treating such nonsteady-state reflected-wave signals, which is applicable when the observed transient behaves as if caused by a lumped-parameter system, is the Prony[3] method. Such behavior arises primarily in panels of small overall thickness, so that the majority of the reflected-wave transient is caused by the turnon transient of the source of the interrogating wave.

As panel thickness is increased, the sample behaves increasingly as a distributed-parameter system, so that the Prony method is no longer applicable to the reflected waveform. The ONION method[4,5] is ideally suited to samples that behave as a distributed-parameter system; i.e., samples whose reflected wave contains significant transients that are associated with the round-trip travel times of waves in the panel sublayers. This method is a reflection-coefficient measurement technique that is designed for use on thick underwater acoustic panels in the frequency range 1–10 kHz, but may be used to frequencies as high as 25 kHz. The approach is based on least-squares fitting of a multiple-layer panel model to the measured reflected-pulse waveform. For a complete description of the method, see Ref. 4.

The initial development of the ONION method was restricted to the analysis of reflected-wave data acquired by probing the sample with an interrogating wave that arrives at normal incidence to the panel. However, since the reflection coefficient is a function of incidence angle, it is of interest to determine sample behavior as a function of measurement angle. The present article examines a generalization of the ONION method to allow for offnormal incidence angles.

Section I presents a synopsis of the approach. A discussion of geometry, edge waves, and certain ramifications of the theoretical panel model is presented in Sec. II. This section also describes how angular interpolations and extrapolations are achieved. A description of experimental measurements made to investigate the effectiveness of the method is given in Sec. III. Section IV gives a discussion of the meaning of the measurements obtained, and also presents a description of some potential influences of certain experimental aspects that represent departures from the ideal conditions assumed by theory. A summary and the conclusions are given in Sec. V.

Throughout this paper, it is assumed that the reader is thoroughly familiar with the ONION method as applied to the normal-incidence case. It is also assumed that the reader understands the structure and behavior of an underwater acoustic panel, and is familiar with the conventional panel-measurement configuration. The reader who is not confident in his knowledge of these subjects is directed to Refs. 1, 2, 4, and 5.

I. BRIEF OVERVIEW OF THE GENERALIZED ONION METHOD

Figure 1 is a block diagram that summarizes the approach used in the generalized ONION method. The algorithm involves three phases. In phase 1, incident and reflected pulsed waveforms experimentally measured at *normal* incidence are used in a normal-incidence ONION-method calculation[4] to obtain starting model parameters. In phase 2, a further least-squares adjustment of the model parameters is performed. During this phase, a simultaneous least-squares minimization of the mean-squared error between the model and the data is performed using all incident and reflected pulsed waveforms that have been measured at each of the incidence angles of interest. The maximum permissible incidence angle is restricted by the requirement to avoid the interfering influence of the sample edge-diffracted wave. (This will be described further in Sec. II B.) Since a restricted range of incidence angles is considered, it is assumed that a *fluid*-layer panel model may be used in the fitting process. (Justifications for this assumption are presented in Sec. II C.) Phase 2 is iterated several times to achieve model parameters that are most consistent (in a least-squares sense) with the experimental data.

Once the "best-fit" parameter values have been determined by phase 2, these parameter values are substituted into a *solid*-layer panel model, during phase 3, to deduce reflection coefficients throughout the range of incidence angles from 0 to 89 deg. (The 90-deg direction is omitted to avoid a numerical singularity in the available software that performs the calculation.) In using the solid-layer model, *a priori* values of the shear properties of the layers are assumed. In most cases of measurement interest, however, it is assumed that the materials of the panel layers are characterizable by negligible shear; it is assumed that only the steel backing plate contributes a significant shear effect. The phase 3 portion of the algorithm, which implements the solid-layer panel model calculation just described, computes reflection coefficients that interpolate between measurement angles and that extrapolate beyond the greatest available measurement angle.

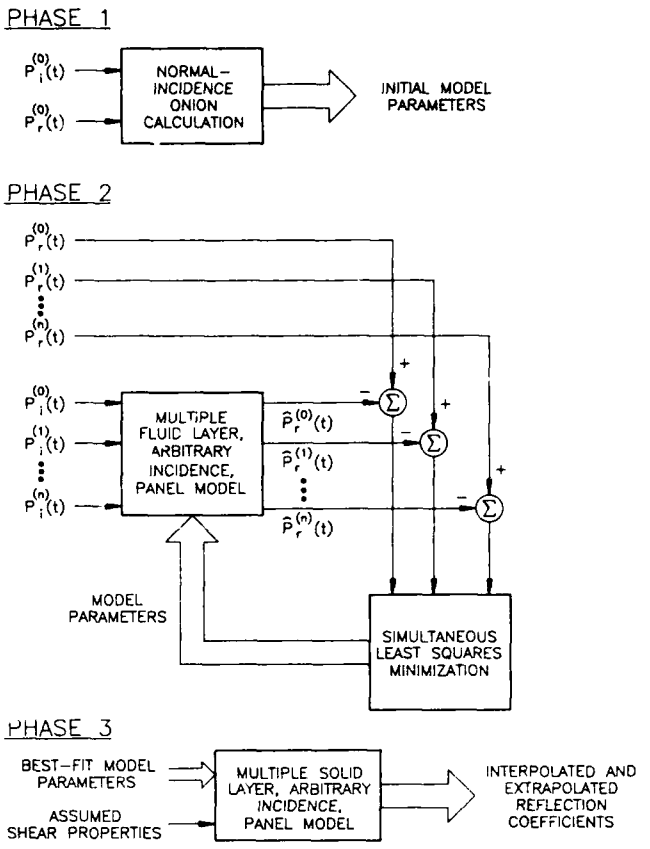

FIG. 1. Block diagram of the generalized ONION-method algorithm. The algorithm involves three phases. In phase 1, the experimentally measured incident pulsed waveform at *normal* incidence $p_i^{(0)}(t)$, and the resulting experimentally measured reflected pulsed waveform $p_r^{(0)}(t)$, are used in a normal-incidence ONION-method calculation to obtain starting model parameters. In phase 2, the model parameters obtained from phase 1 are iteratively improved using a nonlinear least-squares fitting procedure that simultaneously fits an offnormal incidence theoretical panel model to data acquired at all measurement angles. A *fluid*-layer panel model is used during this phase. Finally, in phase 3, the best-fit model parameters deduced by phase 2 are used together with assumed shear properties for the layers in a calculation based on a *solid*-layer panel model to obtain interpolated and extrapolated reflection coefficients as a function of incidence angle θ. Here, $p_i^{(n)}(t)$ represents the experimentally-measured incident pulsed time waveform at the nth incidence angle ($n = 0$ represents normal incidence); $p_r^{(n)}(t)$ represents the experimentally measured reflected pulsed time waveform at the nth incidence angle; and $\hat{p}_r^{(n)}(t)$ is the computed reflected pulsed time waveform at the nth incidence angle, based on a multiple fluid-layer panel model.

II. CALCULATIONAL CONSIDERATIONS

A. Geometry

Figure 2 depicts the measurement configuration used for acquiring reflected-wave data in an offnormal-incidence panel measurement. In this figure, d_s is the distance separating the source and the rotator shaft that supports the test panel. The quantity d_h represents the offset distance of the detector hydrophone from the first layer, i.e., the layer closest to the hydrophone. The hydrophone is rigged so that it corotates with the test panel; i.e., it remains centered with respect to the panel's edges. The quantity t is the overall sample thickness. The angle ϕ, which is depicted in the figure as the angular location of the hydrophone with respect to the acoustic axis, also represents the rotator shaft angle that is adjusted during measurement. The angle θ represents the incidence angle for specularly reflected waves.

It is important to note that the angles θ and ϕ are generally unequal. A trigonometric calculation shows that

$$\theta = \tan^{-1}\left(\frac{d_s \sin\phi}{d_s \cos\phi - t + d_h}\right). \tag{1}$$

For a panel measurement as performed in the Anechoic Tank Facility (ATF) of the Underwater Sound Reference Detachment of the Naval Research Laboratory (NRL-USRD) in Orlando, Florida, a conventional configuration uses values of $d_s = 170$ cm and $d_h = 34$ cm. For a panel of thickness $t = 15$ cm and a rotator shaft measurement angle of $\phi = 45°$, Eq. (1) yields an incidence angle of $\theta \approx 40.8°$; thus a considerable angular error can be made if θ and ϕ are

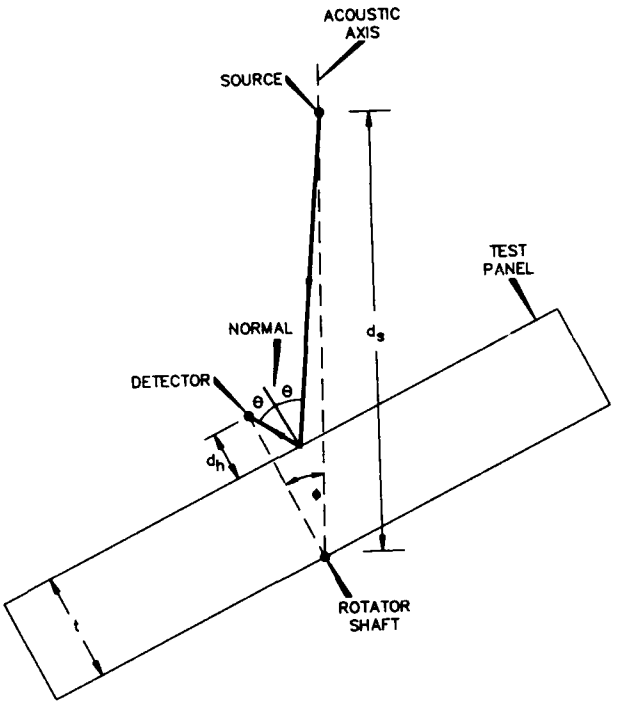

FIG. 2. Diagram depicting the geometry of an offnormal-incidence panel measurement configuration. The figure presents a top view; i.e., from directly above the test panel. Here, d_s represents the source-to-rotator shaft separation distance; d_h represents the hydrophone offset distance from the first panel layer (i.e., the panel layer closest to the hydrophone); t represents the total panel thickness; ϕ represents the rotator shaft angle; and θ represents the incidence angle for specular reflection.

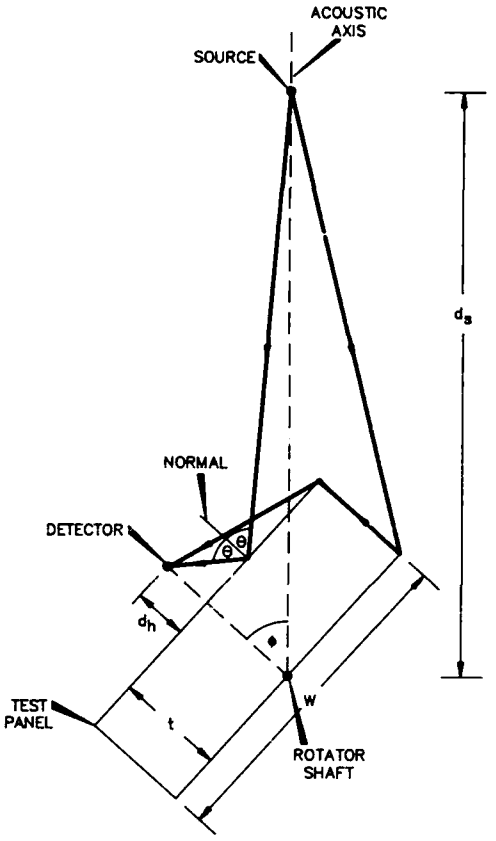

FIG. 3. Diagram depicting acoustic ray paths for the specularly reflected wave and the edge-diffracted wave arising from the steel backing plate. The figure presents a top view; i.e., from directly above the test panel. Variables are the same as those used in Fig. 2. The additional variable w represents the width of the sample panel (assumed to have a square cross section).

assumed to be identical. It is interesting to note, however, that if the hydrophone offset is equal to the panel thickness, i.e., if $d_h = t$, then Eq. (1) reduces to $\theta = \phi$ for all measurement angles.

Typical values of the measurement variables of Fig. 2 as used in ONION-method measurements are $d_s = 200$ cm and $d_h = 5$ cm. For a panel of $t = 15$ cm overall thickness and a measurement angle of $\phi = 45°$, Eq. (1) leads to the value $\theta \approx 47.1°$. Note that θ exceeds ϕ for the typical configuration used in ONION-method measurements, while θ is less than ϕ for the typical configuration used in conventional measurements. This difference in behavior is primarily due to the different hydrophone offsets d_h used in each configuration.

It is also important to realize that for panels containing layers composed of deformable materials, the overall panel thickness t will vary as a function of hydrostatic test pressure. (The hydrophone offset d_h will also change; this will be discussed further in the following subsection.) Thus Eq. (1) will yield a different incidence angle θ for the same rotator shaft angle ϕ at different hydrostatic test pressures.

B. Edge waves and data windows

Since the theoretical model used to deduce the reflected pulsed waveform in the ONION method neglects wave contributions arising from the sample edges, it is important to choose data "windows" that admit into the analysis only data that are not significantly corrupted by panel-edge diffraction. Unfortunately, due to the relatively low sound speeds and relatively large thicknesses of samples of measurement interest, it is usually not possible to entirely exclude contributions from panel-edge waves. However, this problem is not severe due to the fact that the initial sample layers (i.e., those closest to the hydrophone) typically have a good acoustic "match" to the surrounding water medium, and the interrogating wave has a turnon transient; hence, initial edge-wave contributions tend to be of rather low amplitude. On the other hand, the edge wave due to the steel backing plate that is typically affixed to test panels can be rather large in amplitude; thus the data window is selected to avoid edge-wave contributions associated with the backing plate.

In view of the fact that the materials used to fabricate sample panels are typically characterized by sound speeds less than that of the surrounding water medium, it is usually the acoustic path through the water medium that represents the least time-of-flight between any two points of interest in a panel measurement. A typical source-to-backing plate-to-detector path, and the specularly reflected path, are depicted in Fig. 3.

In terms of the variables of Fig. 3, we can deduce expressions for the path length of the specularly reflected wave δ_{spec} and the path length of the edge-diffracted wave δ_{edge} arising from the backing plate. The expressions are

$$\delta_{spec} = [(d_h + d_s \cos\phi - t)^2 + (d_s \sin\phi)^2]^{1/2}, \quad (2)$$

and

$$\delta_{edge} = \{[(w/2)\cos\phi]^2 + [d_s - (w/2)\sin\phi]^2\}^{1/2} + t + [(w/2)^2 + d_h^2]^{1/2}, \quad (3)$$

where w represents the sample width (the sample is assumed to have a square cross section). In applying Eqs. (2) and (3), it should be realized that when hydrostatic test pressure is increased, overall panel thickness[6] t decreases, while the hydrophone offset d_h undergoes a corresponding increase. This is so because the hydrophone is rigged to maintain a fixed distance from the rotator shaft, but the quantity d_h is measured with respect to the front panel face. This panel face recedes from the hydrophone as hydrostatic test pressure is increased. The two effects (i.e., increasing d_h and decreasing t) tend to decrease the acoustic path difference $\delta_{edge} - \delta_{spec}$. Hence, if a single data window width is to be used at a given measurement angle for all hydrostatic test pressures, a conservative approach is to use the window width that eliminates the edge-wave contribution at the greatest hydrostatic test pressure of interest.

For example, imagine a sample panel whose overall thickness t is 15 cm at atmospheric pressure, but which decreases to 12.5 cm at the greatest hydrostatic test pressure of interest. (Such a compression is realistic for the panels of measurement interest.) Imagine also that the rotator shaft angle of interest is $\phi = 20°$. It is convenient in the calculations that follow to imagine that the incident and reflected wave data are acquired in digital form, as required by the ONION-method algorithm. Let us take the digital data acquisition rate to be 4 MHz, and calculate the corresponding number of reflected-wave data points in the data window that avoids contributions from the edge-diffracted wave arising from the steel backing plate. This number of points is calculated from the formula

$$\begin{pmatrix}\text{number of}\\ \text{points}\end{pmatrix} = \begin{pmatrix}\text{data}\\ \text{measurement}\\ \text{rate}\end{pmatrix} \times \left(\frac{\delta_{edge} - \delta_{spec}}{c_0}\right), \quad (4)$$

where c_0 is the speed of sound in the surrounding water medium. Assuming a hydrophone offset of $d_h = 5$ cm at atmospheric pressure, a water sound speed of $c_0 = 1.5 \times 10^5$ cm/s, and a 4-MHz data measurement rate, Eq. (4) yields a data window width of 1435 points at $\phi = 20°$, assuming a sample width of $w = 76$ cm (30 in.). However, recalculating the data window width using the 12.5-cm thickness assumed for the higher hydrostatic test pressure results in a window width of 1250 points. (In this calculation, a hydrophone offset of $d_h = 7.5$ cm must be used; i.e, the 5-cm offset given for atmospheric pressure must be increased by an amount equal to the corresponding decrease in sample thickness, which is $15 - 12.5 = 2.5$ cm in this example.) Thus to avoid[7] the edge wave from the backing plate at all hydrostatic test pressures of interest requires a window width of no greater than 1250 points at the rotator shaft angle $\phi = 20°$.

C. Model considerations

The theoretical model used in the *normal*-incidence implementation of the ONION method[4,5] treats each panel layer as a fluid; i.e., it is assumed that the shear modulus of each layer is negligible. This simplification is readily justifiable in the normal-incidence case. Panel layers in samples of interest are generally fabricated in a manner that creates in each layer an array of air-filled macrovoids in a rubber matrix material. Both air and rubber are characterized by quite low values of the shear modulus. Of course, the test panel is typically affixed to a support plate fabricated from steel, a material having a very significant shear modulus. However, it should be noted that no shear waves are excited in a solid of infinite lateral extent that is stimulated by a normally incident interrogating wave. The influence of the edges of a finite sample can be reduced by acquiring the measurements in the pulsed mode, and gating out edge effects. Hence, even the steel backing plate can accurately be modeled as a fluid in the normal-incidence case.

As the interrogating wave incidence angle is allowed to deviate from the normal, however, shear-wave production becomes increasingly significant, so that it is possible that the steel backing plate may no longer be accurately treated as a fluid. (Due to the very low values of the shear modulus of the materials constituting the macrovoided viscoelastic layers, however, it is assumed that shear-wave production will remain insignificant for these layers even at large offnormal incidence angles.)

The influence of shear-wave production in a steel backing plate can be seen by examining Table I. This table presents complex reflection coefficients as a function of incidence angle for a single layer of steel and for a single layer of a steel-like fluid. [In this table, and the following tables, the real and imaginary parts of the complex reflection coefficient are presented using the complex-number convention (real, imaginary).] The steel-like fluid is taken to have a

TABLE I. Complex reflection coefficients as a function of incidence angle for a single layer of steel and for a single layer of a steel-like fluid. The steel-like fluid is taken to have a density equal to that of steel and to have a longitudinal sound speed equal to the longitudinal wave speed in steel. In both cases, the sample is immersed in an infinite water medium. Frequency is 20 kHz. Sample thickness is 0.95 cm ($\frac{3}{8}$ in.).

Incidence angle θ (degrees)	Complex reflection coefficient (dimensionless) Steel	Steel-like fluid
0	0.906,0.289	0.906,0.289
5	0.905,0.290	0.905,0.290
10	0.904,0.292	0.903,0.294
15	0.900,0.304	0.899,0.301
20	0.895,0.301	0.894,0.311
25	0.887,0.312	0.886,0.325
30	0.873,0.327	0.875,0.341
35	0.855,0.348	0.861,0.362
40	0.826,0.374	0.843,0.386
45	0.785,0.405	0.819,0.415

negligible shear modulus (corresponding to a shear wavespeed of 1 m/s) and is taken to have the same density as steel and to have a longitudinal sound speed equal to the longitudinal wavespeed in steel. In both cases, the layer is assumed to be immersed in an infinite water medium. Frequency is 20 kHz and sample thickness is 0.95 cm ($\frac{3}{8}$ in.). This thickness corresponds to the thickness of a standard support plate typically used in a panel test. The 20-kHz frequency considered is close to the maximum 25-kHz frequency for which ONION-method measurements are intended.

Perhaps the most striking feature of Table I is that the values presented for steel actually deviate very little from those presented for the steel like fluid, at least for incidence angles less than 30°. This behavior is also typical of that seen for the lower test frequencies of 5 and 10 kHz that were considered, but which are not presented here. (In fact, the deviation is even less for frequencies less than 20 kHz.) This behavior is probably caused by the small layer thickness of 0.95 cm that was used in the calculation. However, since the thickness used in the calculations that generated Table I represents the thickness of a standard support plate, and in view of the rather low shear modulus characteristic of the materials that constitute the layers of test panels, the results presented in Table I are taken as a justification of the continued use of a fluid-layer model to analyze offnormal incidence measurements in the phase 2 portion of the generalized algorithm, at least for incidence angles θ less than 30°. (In fact, θ is restricted to be less than or equal to that incidence angle that corresponds to a rotator shaft angle of $\phi = 20°$ in the calculations in which a fluid-layer model is used. This angular restriction is used to avoid the edge wave from the steel backing plate.) The motivation for using a fluid-layer model rather than the more accurate solid-layer model during the phase 2 portion of the method is to avoid the significant increase in computer processing time that would result from using a solid-layer model.[8]

The validity of the fluid-layer model for offnormal incidence can be further investigated by referring to the results presented in Tables II–IV. These tables present information similar to that presented in Table I, except in these tables the sample considered consists of three homogeneous sublayers" instead of the single steel layer considered in Table I. In this sample, the layer closest to the sound source is composed of polymethylmethacrylate (PMM) of 2.54-cm (1-in.) thickness, the second layer is a water layer of 2.54-cm (1-in.) thickness, and the third layer is steel layer of 0.95-cm ($\frac{3}{8}$-in.) thickness. The column labeled "solid layers" presents complex reflection coefficients evaluated by treating the PMM and steel layers as solids. The results presented in the column labeled "fluid layers" were obtained by treating the PMM and steel layers as having a negligible shear modulus. In addition, the density of each of these layers was taken equal to that in the corresponding solid layer, and the longitudinal sound speed in each of these layers was taken equal to the longitudinal wave speed of the corresponding solid layer.

As can be seen by referring to Tables II and III, the results for the solid-layer and fluid-layer cases are very similar to each other for the frequencies 5 and 10 kHz, at least for incidence angles less than or equal to 20°. The deviation is greater for the 20-kHz case, as can be seen by referring to Table IV, and is particularly so for $\theta = 15°$. Note, however,

TABLE III. Complex reflection coefficients as a function of incidence angle for a simple three-layer sample. Frequency is 10 kHz.

Incidence angle θ (degrees)	Complex reflection coefficient (dimensionless) Solid layers	Fluid layers
0	0.582,0.509	0.582,0.509
5	0.587,0.497	0.591,0.492
10	0.603,0.457	0.616,0.436
15	0.627,0.383	0.648,0.336
20	0.643,0.263	0.666,0.182
25	0.671,0.126	0.633,0.029
30	0.641,0.057	0.496,0.270
35	0.565,0.238	0.206,0.458
40	0.448,0.391	0.192,0.457
45	0.314,0.494	0.527,0.206

TABLE II. Complex reflection coefficients as a function of incidence angle for a simple three-layer sample. Frequency is 5 kHz.

Incidence angle θ (degrees)	Complex reflection coefficient (dimensionless) Solid layers	Fluid layers
0	0.524,0.218	0.524,0.218
5	0.525,0.213	0.527,0.211
10	0.530,0.200	0.535,0.189
15	0.542,0.169	0.548,0.152
20	0.491,0.218	0.560,0.100
25	0.521,0.161	0.569,0.033
30	0.521,0.116	0.570,0.047
35	0.513,0.080	0.558,0.138
40	0.496,0.045	0.528,0.235
45	0.470,0.014	0.477,0.335

TABLE IV. Complex reflection coefficients as a function of incidence angle for a simple three-layer sample. Frequency is 20 kHz.

Incidence angle θ (degrees)	Complex reflection coefficient (dimensionless) Solid layers	Fluid layers
0	0.974,0.164	0.974,0.164
5	0.972,0.172	0.971,0.182
10	0.966,0.203	0.960,0.236
15	0.224,0.970	0.936,0.319
20	0.937,0.305	0.893,0.425
25	0.871,0.459	0.825,0.546
30	0.694,0.697	0.727,0.671
35	0.181,0.970	0.597,0.788
40	0.858,0.512	0.431,0.887
45	0.462,0.846	0.224,0.954

that this sample represents a rather severe test of the fluid-layer model, in view of the significant shear modulus and thickness of the PMM layer. If the shear modulus of the PMM layer is permitted to decrease to an insignificant value, while retaining the true shear modulus in the steel layer and the true longitudinal wave speed for PMM, agreement with the fluid-layer case is substantially improved. (This calculation is of interest since the materials used in panels of actual measurement interest have a substantially lower shear modulus than that of PMM.) Table V presents results for the 20-kHz case in which the PMM layer is treated as a fluid but the steel layer is treated as a solid. As can be seen by comparing Table V with the fluid-layer column of Table IV, agreement is considerably improved, even at $\theta = 15°$. In view of the fact that the situation considered in generating the results displayed in Table V more closely represents the situation of actual measurement interest than the situation considered in generating the solid-layer results of Table IV, we take the above-mentioned agreements as establishing the validity of the fluid-layer model, at least for frequencies less than or equal to 20 kHz and for incidence angles corresponding to rotator-shaft angles that are less than or equal to 20°. The validity of this assumption is also further investigated in the description of the experiments presented in Sec. III.

D. Angular interpolation and extrapolation

Based on the calculations described in the preceding subsection, and based on the verifying measurements to be described in Sec. III, it is assumed that the phase 2 portion of the ONION-method algorithm for offnormal incidence can be accurately implemented in software that treats the layers of the panel as fluids. Once the best-fit properties have been determined in this manner, the phase 3 portion of the algorithm performs a calculation of the reflection coefficient magnitude as a function of incidence angle. This calculation is done by using the best-fit model properties that have been determined during phase 2, as well as using assumed shear properties for the layers, in a solid-layer panel model. This calculation is performed for an angular range of 0–89 degrees at increments of 1°. (As previously mentioned, the $\theta = 90°$ direction is omitted in order to avoid a numerical singularity at that angle in the available software.) Computed reflection coefficients for incidence angles falling between measurement angles represent interpolated values. Computed reflection coefficients for incidence angles greater than the largest measured incidence angle represent extrapolated values. In evaluating samples containing macrovoided viscoelastic layers, it is only the steel support plate that is assumed to have a significant shear modulus. Hence, negligible values of the shear modulus[10,11] are used for the macrovoided viscoelastic layers when this final calculation[12] is made. In view of the fact that this final calculation only needs to be performed once for each measured frequency, only an insignificant amount of CPU time is required for it. Thus total computation time is not significantly increased by this use of the full solid-layer model in the phase 3 calculation.

If a significant shear-wave effect, due to the support plate, arises at large offnormal-incidence angles, it is assumed that this effect will manifest itself in the final phase 3 calculation. This idea can be seen by examining Fig. 4(a) and (b). These figures present graphs of the theoretical magnitude of the reflection coefficient as a function incidence angle for the simple three-layer panel discussed above, evaluated here for a 20-kHz interrogating wave. Figure 4(a) presents results based on treating all three layers as fluids; Figure 4(b) presents results based on treating both the PMM and steel layers as solids. The considerable influence of shear waves in this case can be seen in the significant differences between these two graphs at the larger incidence angles. Note, however, that the graphs are virtually indistinguishable at small incidence angles. This is an indication that it should be possible to perform a least-squares fit of a fluid-layer model, as is required in the phase 2 portion of the generalized ONION algorithm, to data acquired from such a sample, at least for incidence angles that are less than or equal to the incidence angle that corresponds to a rotator shaft angle of 20°. After the fitting process (based on the data acquired at the measured angles) is complete, a curve closely corresponding to Fig. 4(b) (i.e., the solid-layer curve) can be generated, assuming that accurate shear properties are available for each of the layers of the panel. This is what is done in the phase 3 portion of the algorithm.

TABLE V. Complex reflection coefficients as a function of incidence angle for a simple three-layer sample. Here, PMM is treated as a fluid, while steel is treated as a solid. Frequency is 20 kHz.

Incidence angle θ (degrees)	Complex reflection coefficient (dimensionless) Fluid PMM–water–solid steel
0	0.974,0.164
5	0.971,0.182
10	0.960,0.235
15	0.936,0.320
20	0.893,0.424
25	0.825,0.544
30	0.728,0.668
35	0.597,0.785
40	0.430,0.883
45	0.221,0.946

III. EXPERIMENTS

A. Simple three-layer sample

In order to provide a basis for an initial investigation of the effectiveness of the generalized ONION method, experimental data were acquired from a simple three-layer sample panel. This is the same sample as was used in the initial testing of the normal-incidence ONION method,[4,5] and is the same panel that was considered theoretically in Sec. II (C) and (D).

Data were acquired from this sample at interrogating-wave frequencies of 5, 10, and 20 kHz. Both normal and offnormal incidence measurements were made. The rotator-shaft angles ϕ that were used[13] in these measurements are 0°,

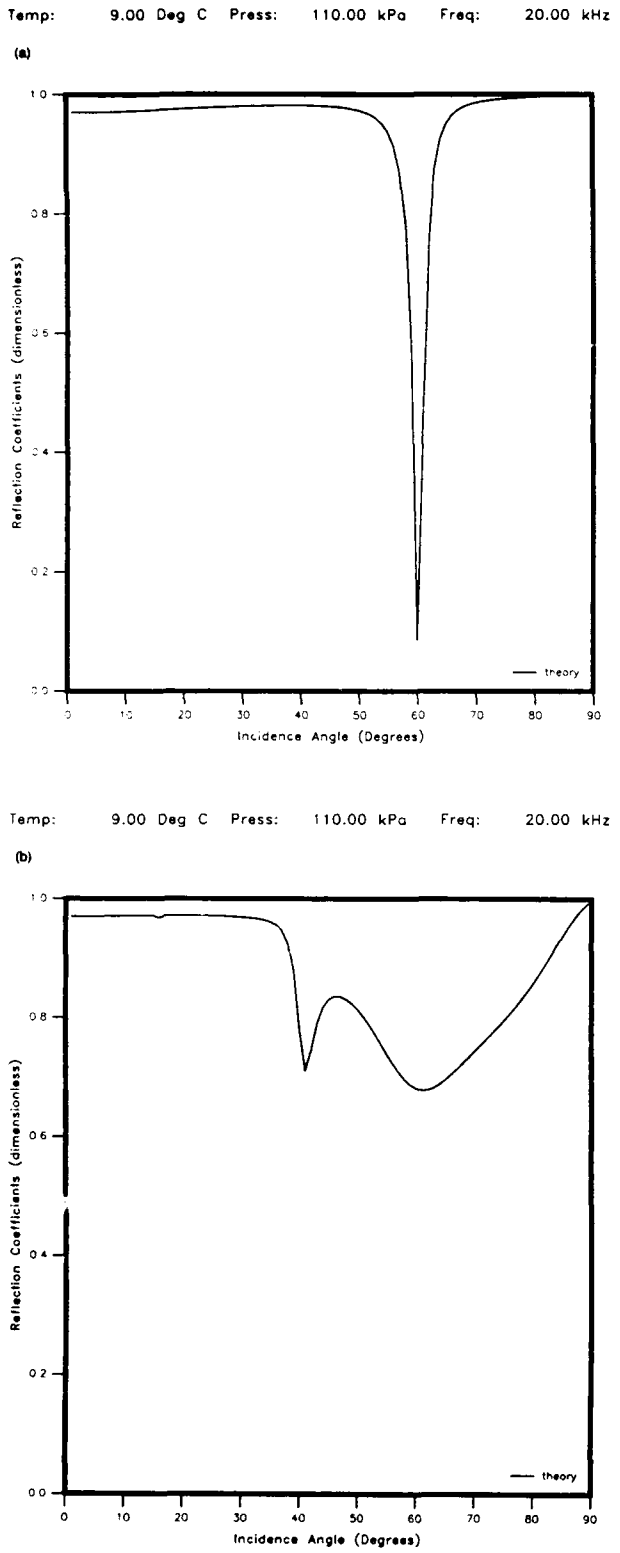

FIG. 4. Theoretical reflection coefficient magnitude as a function of incidence angle θ for the simple three-layer panel. Frequency is 20 kHz. (a) All panel layers treated as fluids. (b) PMM and steel layers treated as solids.

5°, 10°, 15°, and 20°. A hydrophone offset distance of $d_h = 5$ cm from the PMM layer, and a source-to-rotator-shaft separation distance of $d_s = 200$ cm, were used in this experiment.

The results of these measurements, and of applying the generalized ONION method algorithm to the data, are summarized by the graphs presented in Fig. 5. The dashed-line curves in the graphs presented in these figures represent the final output of the software based on the phase 3 portion of the method; thus the dashed-line curves were generated by using the best-fit values produced by the least-squares fitting process of phase 2, as well as the known shear properties of PMM and steel, in a solid-layer model calculation. The solid circles that are plotted on top of these dashed-line curves are reference points that are used to indicate the incidence angles θ that correspond to the measurement angles ϕ at which the data were acquired. Hence, portions of the dashed-line curves lying between the solid circles represent interpolated reflection coefficients, while portions of the dashed-line curves lying beyond the last solid circle represent extrapolated reflection coefficients.

The effectiveness of the method in this case can be ascertained by reference to the solid-line curves in Fig. 5. These curves were generated by using the known properties of PMM, water, and steel in a theoretical calculation based on the solid-layer panel model. As can be seen by comparing the solid-line and dashed-line curves in Fig. 5, the experimental and theoretical curves are in good agreement at 5 and 10 kHz, with the exception of the peak in the vicinity of $\theta = 38°$ in the 5-kHz curves. There is even a reasonable agreement in the qualitative features of the curves based on the 20-kHz case, despite the fact that this frequency might have been anticipated to be troublesome for this sample. (Note again Table IV.) In particular, note that the extrapolation region of the dashed-line curve presented in Fig. 5(c) (i.e., the region beyond the last solid circle in this figure) successfully predicts the "notch" in the vicinity of $\theta = 40°$ of the 20-kHz theoretical curve (solid line); however, the reflection coefficient corresponding to the bottom of the notch is incorrectly predicted by approximately 14%. Quantitative agreement between the dashed-line and solid-line curves of Fig. 5(c) is poorest beyond approximately $\theta = 50°$, although the qualitative features are similar. Nonetheless, in view of the fact that the data were measured only up to a rotator-shaft angle of $\phi = 20°$, the extrapolation represents a considerable increase in the amount of available information. Considering the fact that this panel, and particularly the 20-kHz frequency case, represents an especially severe test of the fluid-layer panel model used in the phase 2 portion of the method, the results of this measurement can reasonably be described as encouraging.

B. Panel containing macrovoided viscoelastic layers

Experimental data were next acquired from a sample panel containing macrovoided viscoelastic layers. This is the same sample described in the reports of the normal incidence work.[4,5,14] A hydrophone offset distance of $d_h = 5$ cm, and source-to-rotator shaft separation distance of $d_s = 200$ cm, were used in performing these measurements. The interrogating-wave frequencies were again 5, 10, and 20 kHz, and the hydrostatic test pressures used were atmospheric pressure and 1380 kPa (200 psi). Rotator shaft measurement angles ϕ were 0°, 5°, 10°, 15°, and 20°.

The results of applying the generalized ONION-meth-

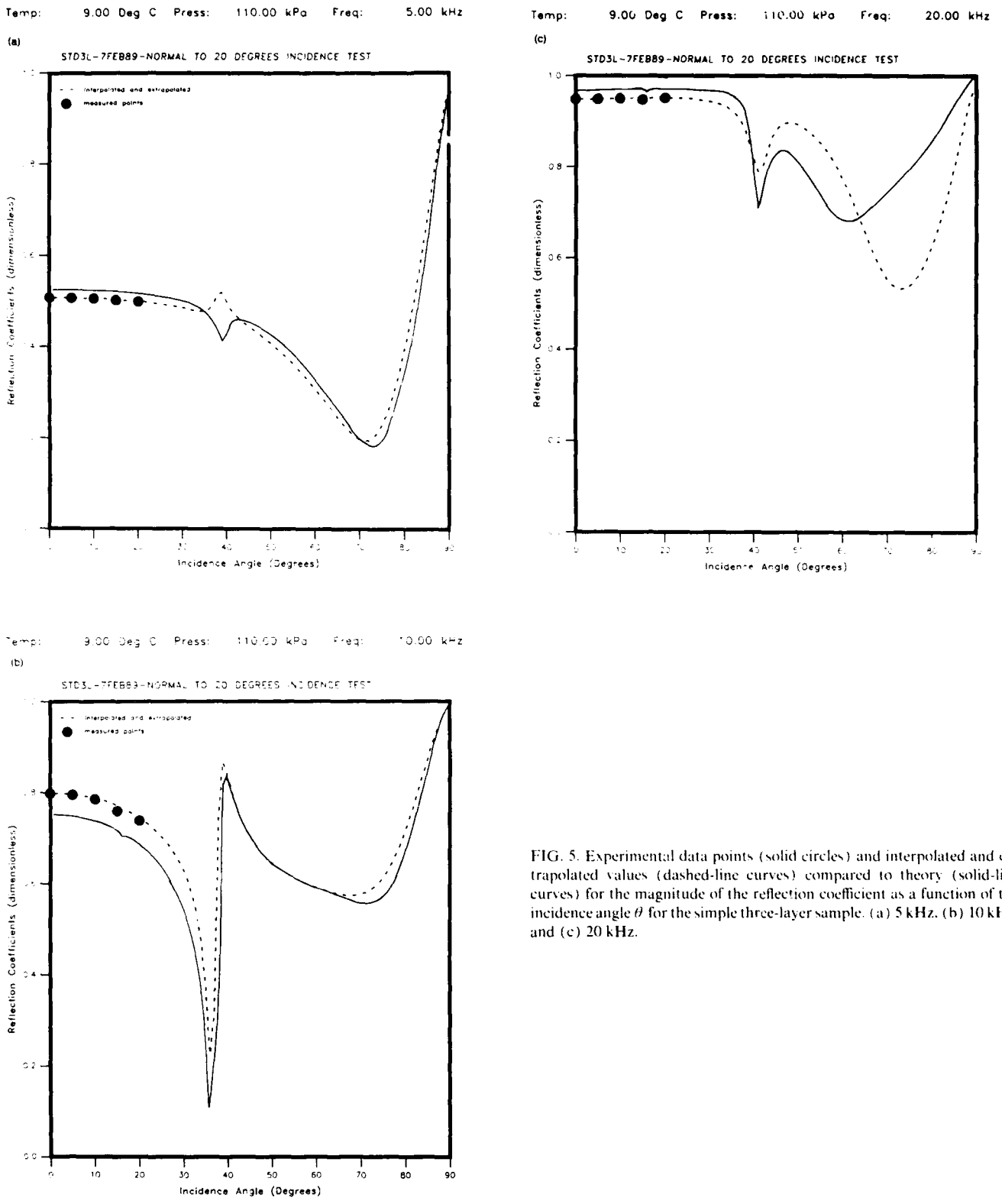

FIG. 5. Experimental data points (solid circles) and interpolated and extrapolated values (dashed-line curves) compared to theory (solid-line curves) for the magnitude of the reflection coefficient as a function of the incidence angle θ for the simple three-layer sample. (a) 5 kHz, (b) 10 kHz, and (c) 20 kHz.

od algorithm to these measurements are summarized in Figs. 6 and 7. Unfortunately, effective sound speeds and losses of the layers comprised by this sample are unknown, so comparison of these results with theory is not possible for this case. Thus, in this case, we examine instead the experimental and model reflected pulsed waveforms, within the appropriate data windows, as a function of rotator shaft angle ϕ. Figure 8 presents these waveforms for the 5-kHz test case measured at the 1380 kPa (200 psi) hydrostatic test pressure.[15] As can be seen, agreement between the model and the data is reasonably good at all angles. This figure is typical of the results obtained at the other test frequencies

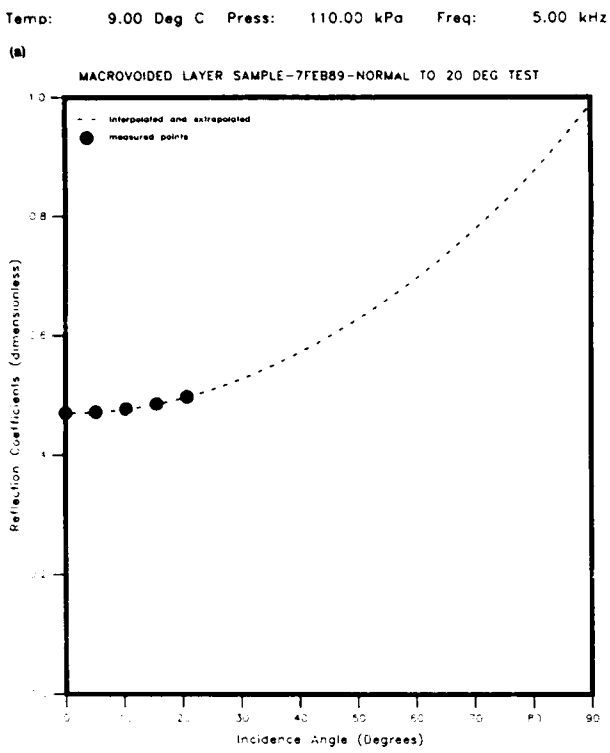

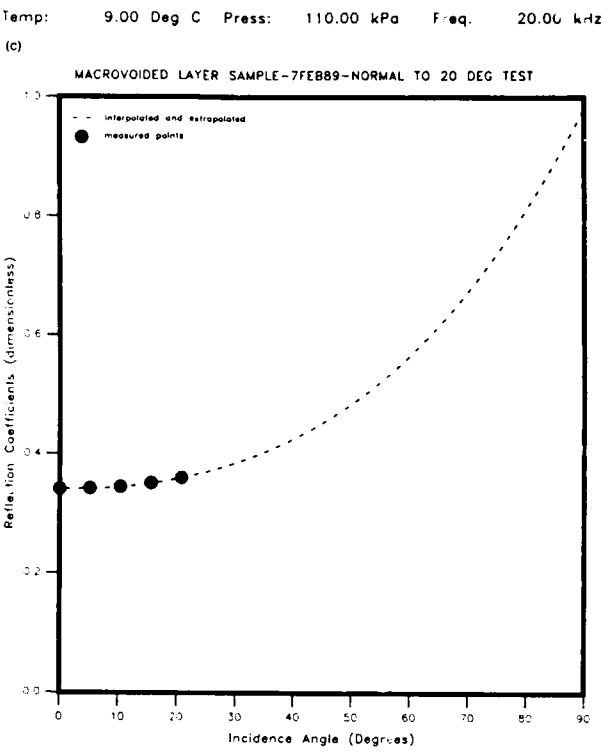

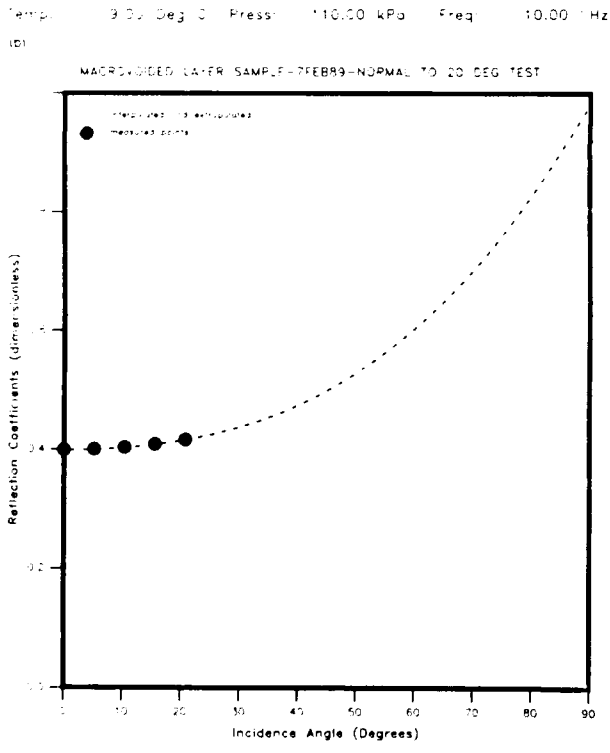

FIG. 6. Experimental data points (solid circles) and interpolated and extrapolated values (solid-line curves) for the magnitude of the reflection coefficient as a function of incidence angle θ for the sample containing macrovoided viscoelastic layers. Hydrostatic test pressure is atmospheric. (a) 5 kHz, (b) 10 kHz, and (c) 20 kHz.

evaluated at this pressure, and is also typical of the results obtained for each of the test frequencies evaluated at atmospheric pressure.

IV. DISCUSSION

While the experimental results presented for the panel containing simple homogeneous layers are in reasonably good agreement with theory, and although the results presented for the panel containing macrovoided viscoelastic layers also exhibit reasonable behavior, some further considerations are necessary to gain an appreciation of the meaning of the results obtained for these measurements. The ONION method is, in essence, an extrapolation procedure; i.e., its purpose is the prediction of steady-state results on the basis

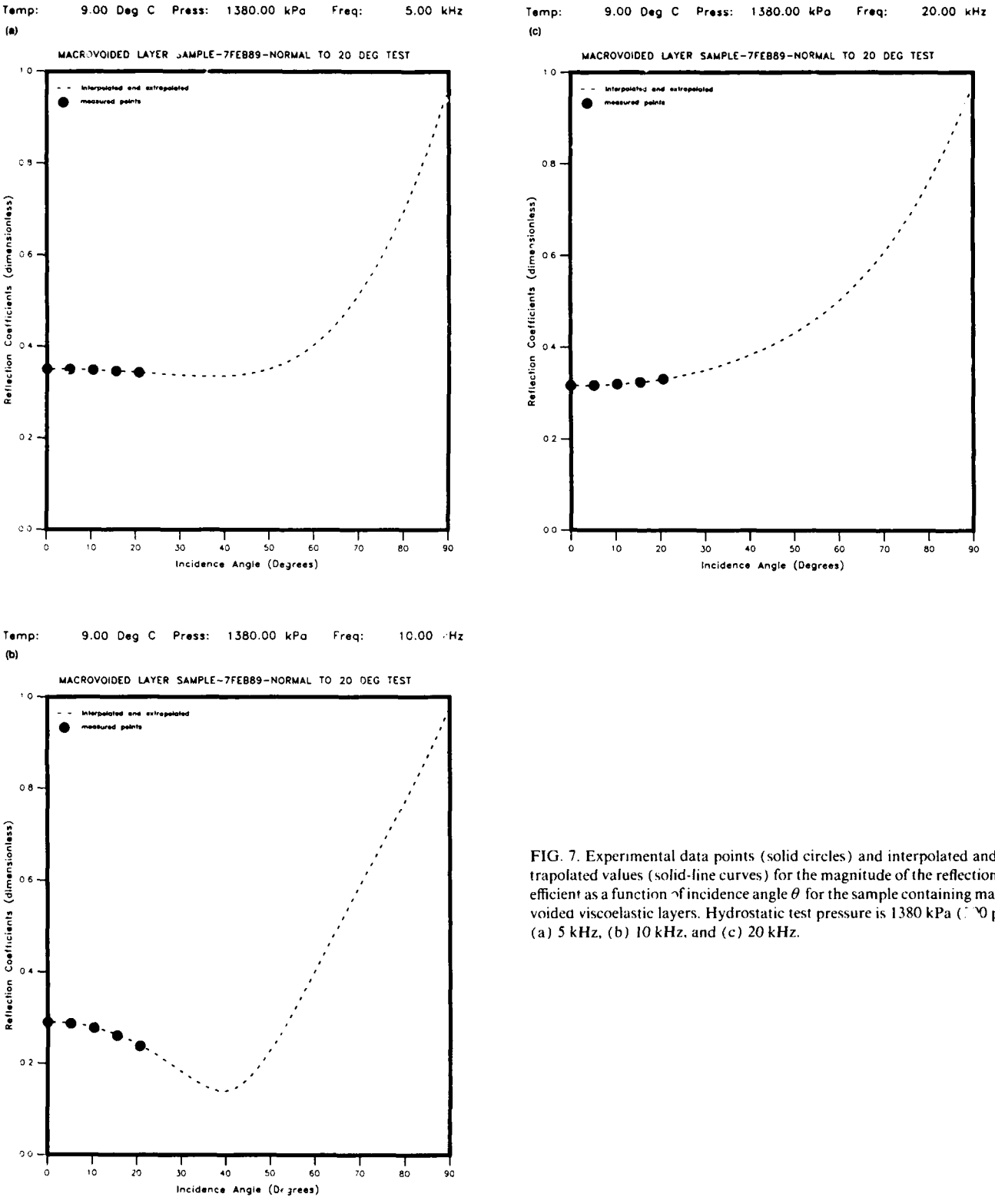

FIG. 7. Experimental data points (solid circles) and interpolated and extrapolated values (solid-line curves) for the magnitude of the reflection coefficient as a function of incidence angle θ for the sample containing macrovoided viscoelastic layers. Hydrostatic test pressure is 1380 kPa (200 psi). (a) 5 kHz, (b) 10 kHz, and (c) 20 kHz.

of available transient-wave data. In the case of offnormal incidence panel measurements, a further extrapolation to incidence angles that are not experimentally realizable (due to the influence of edge effects) is also done. In all cases, the extrapolations are achieved by determining suitable model parameters by performing a least-squares fit of a theoretical model to experimental data.

The theoretical model assumes *effectively* homogeneous layers. Thus inhomogeneities within the materials that form the layers of the sample, and discontinuities represented by the sample edges, are departures of the experimental system from that assumed by the theoretical model. In acquiring experimental data, steps are taken to reduce, as far as possible, the influence of experimental aspects that represent de-

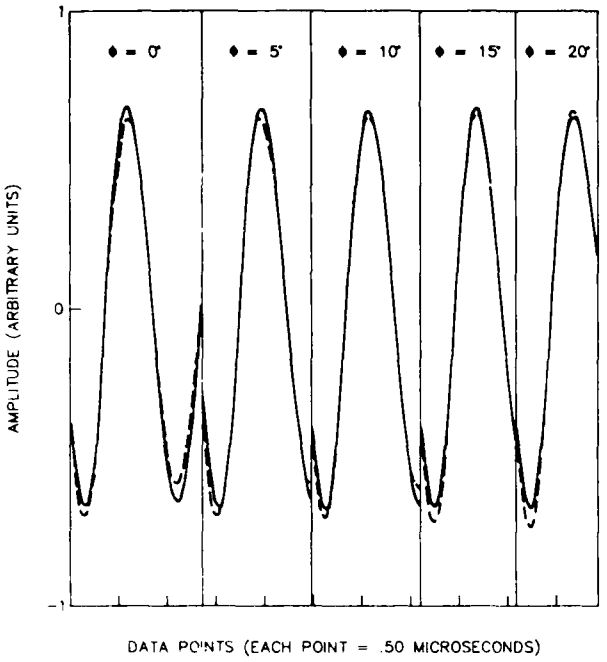

FIG. 8. Experimental reflected pulsed time waveforms (solid lines) and model reflected pulsed time waveforms (dashed lines) at each measured rotator angle ϕ. The portions of the waveforms depicted are the portions used in the data window at each angle. Each data point represents 0.50 μs of time. The width of each data window at each rotator angle is: 519 points at $\phi = 0°$; 474 points at $\phi = 5°$; 427 points at $\phi = 10°$; 380 points at $\phi = 15°$; and 332 points at $\phi = 20°$. (Data windows narrow at increasing rotator shaft angle ϕ to avoid the contaminating edge wave due to the steel backing plate.) Frequency: 5 kHz; hydrostatic test pressure: 1380 kPa (200 psi).

partures from the model. One example of this, previously mentioned, is the use of narrowing data window widths at increasing incidence angles to reduce edge-wave interference.

Each of the macrovoided viscoelastic layers of test panels of interest is usually not fabricated in the form of a single, continuous piece of material. Such layers are usually fabricated from a number of subsections of material. (These subsections are called "tiles.") These tiles typically have the same thickness as the layer to be fabricated, but have a smaller cross-sectional area than that of the panel. (Sometimes several tile thicknesses are laminated together to form the desired layer thickness.) Places where tiles are joined together along their edges in the formation of a panel layer are called "seams." Most panel designs use a random tile-edge arrangement pattern in the fabrication of layers. That is, a variety of tile cross-sectional areas is used in creating an overall layer cross section. This is done in order to reduce the probability that the waves originating at the tile seams will constructively interfere, thereby corrupting the desired measurement. However, neither the random tile geometry, nor the use of narrowing data window widths, entirely eliminates the influences of unwanted interfering waves, and the presence of such waves must be viewed as a contamination of the experimental signal.

One consequence of the presence of contaminating edge waves and seam waves is that such waves will result in errors in the determination of the layer parameters, i.e., sound speeds and losses. However, if the mean-squared error of fit between the model waveform and the experimental waveform can be made small (typically, less than 10%), it is assumed that such errors are not significant. If this assumption is not valid, it might very well mean that any panel measurement made on such a sample is not meaningful. This comment is based on the fact that if, for example, seam waves represent a *significant* component of the observed wave, then the experimentally determined reflection coefficient would be a function of seam geometry and sample size, and this would be true regardless of the method used to perform the measurement. An extrapolation of measurements obtained from a panel having a significant contribution to the observed siginal arising from a random seam geometry would not appear to be a well-posed problem and thus the idea of a panel measurement would not seem to be meaningful in such a case.

An alternate way of viewing the situation is to imagine that the observed wave represents the sum of: (i) a "seam-free field" (i.e., a field characterizable only by the effective medium properties of the layers) and (ii) a "seam field." (In the discussion that follows, we ignore the contribution from panel edge waves.) It is expected that field (i) is independent of sample size and of the details of sample fabrication, but that field (ii) is dependent on each of these factors. The ONION method assumes that the influence of field (ii) is negligible, and that field (i) can be used to characterize the panel. The extent to which this assumption holds is tested within the ONION method by evaluating the fit between the model and the data. It is assumed that if the "goodness-of-fit" should ever happen to fall to some unacceptable level (e.g., worse than 15%) it is due to the influence of a non-negligible field of type (ii). In this case, the extrapolations based on the method would probably be unreliable. However, it would seem that a measurement made in such a case on an ostensibly identical sample (i.e., one fabricated using the same physical layer characteristics as the one originally tested but having a different seam geometry) would have a significantly different experimental response and, hence, the idea of a panel measurement on such a sample is probably meaningless.

V. SUMMARY AND CONCLUSIONS

A generalization of the ONION-method algorithm to allow for offnormal incidence panel measurements has been described. Successful applications of the technique to experimental measurements have also been discussed.

The generalized ONION method involves three phases of calculation. In phase 1, an ordinary normal-incidence ONION calculation determines initial model parameters; in phase 2, a simultaneous least-squares fit of an offnormal incidence fluid-layer panel model to experimental data acquired over a range of incidence angles is performed; in phase 3, the best-fit properties deduced by phase 2, and *a priori* shear properties for the panel layers, are used in a solid-layer panel model calculation to obtain interpolated and extrapolated reflection coefficients as a function of incidence angle.

The experimental measurements that were described here involved a simple three-layer sample as well as a sample containing macrovoided viscoelastic layers. The simple three-layer sample represents a severe test of the fluid-layer panel model used in phase 2, due to the significant shear modulus and thickness of the PMM layer. Agreement between measurements obtained from this sample and theoretical calculations was found to be reasonably good. The results obtained from the sample containing macrovoided viscoelastic layers also exhibit reasonable behavior.

The generalized ONION method assumes that the layers of the sample panel can be characterized using effective medium properties. If actual sample inhomogeneities such as seams and edges produce substantial contributions to the observed field, the extrapolations will probably be unreliable; however, in this case, a panel measurement is probably not meaningful.

The present paper represents an initial investigation into the generalization of the ONION method to offnormal incidence. Future work will seek to establish well-defined regions of applicability of the generalized method, and will further evaluate the possibility of using an effective medium theory to more accurately account for the influence of shear waves.

ACKNOWLEDGMENTS

I am grateful to Dr. A. L. Van Buren for providing a computer program that could readily be modified to produce a subroutine to perform the solid-layer panel calculations required in the phase 3 portion of the algorithm. I am also indebted to Dr. James J. Dlubac of the David Taylor Research Center (DTRC), Bethesda, Maryland, for suggesting that generalizing the ONION method to offnormal incidence would be of value.

[1] R. J. Bobber, *Underwater Electroacoustic Measurements* (U.S. Government Printing Office, Washington, DC, 1970), pp. 294–297. Readers unfamiliar with the standard panel measurement configuration should refer to Fig. 6.2, p. 291, of this reference. See also, Ref. 2.

[2] A. J. Rudgers and C. A. Solvold, "Apparatus independent acoustical-material characteristics obtained from panel-test measurements," J. Acoust. Soc. Am. **76**, 926–934 (1984). Figure 1 presents the basic panel-measurement configuration.

[3] D. H. Trivett and A. Z. Robinson, "Modified Prony method approach to echoreduction measurements," J. Acoust. Soc. Am. **70**, 1166–1175 (1981).

[4] J. C. Piquette, "The ONION method: A reflection coefficient measurement technique for thick underwater acoustic panels," J. Acoust. Soc. Am. **85**, 1029–1040 (1989).

[5] J. C. Piquette, "An extrapolation procedure for transient reflection measurements made on thick acoustical panels composed of lossy, dispersive materials," J. Acoust. Soc. Am. **81**, 1246–1258 (1987).

[6] Layer thicknesses are determined in the ONION method with the help of an underwater video camera. The technique is described in Ref. 4.

[7] Note that for a sufficiently small rotator shaft angle ϕ, the acoustic wave traveling from the source to the backing plate would actually either have to pass through the material of the panel, or have to diffract around the sample edge, rather than taking the direct path depicted in Fig. 3. Due to the fact that the wave speed in panel materials is less than that of water in most cases of measurement interest, and that the path length traveled by the diffracted wave is greater than the direct path, either of these alternative possibilities would require a greater propagation time than that for the path depicted in Fig. 3. Hence, using Eq. (4), which is based on the paths depicted in Fig. 3, to determine the relevant window width, even for small rotator shaft angles ϕ, is a more conservative approach than using the true acoustic path for the situation.

[8] The mathematical expressions needed to evaluate the reflection coefficient for both the fluid-layer model and the solid-layer model can be found in W. T. Thomson, "Transmission of elastic waves through a stratified solid medium," J. Appl. Phys. **21**, 89–93 (1950). (Please note some of the equations in this reference contain misprints.) The solid-layer model requires the multiplication of 4×4 matrices, one for each layer, while the fluid-layer model permits the use of a 2×2 matrix for each layer. The 2×2 matrices require approximately $\frac{1}{4}$ the CPU time that is required to evaluate the 4×4 matrices.

[9] This simple three-layer panel is the same as that considered in Refs. 4 and 5.

[10] The negligibility of shear-wave contributions for a viscoelastic sample is also supported by experimental measurements made for other geometries. See, for example, C. M. Davis, L. R. Dragonette, and L. Flax, "Acoustic scattering from silicone rubber cylinders and spheres," J. Acoust. Soc. Am. **63**, 1694–1698 (1978).

[11] Instead of simply assuming a negligible shear modulus, it may be possible to use an *effective* shear modulus for the macrovoided viscoelastic layers based on one of the many available effective medium theories. For an example of one of these, see the summary provided in G. C. Gaunaurd and W. Wertman, "Comparison of effective medium theories for inhomogeneous continua," J. Acoust. Soc. Am. **85**, 541–554 (1989). However, in view of the fact that effective medium theories are somewhat controversial [see the article, which accompanies the one mentioned above, by L. W. Anson and R. C. Chivers, "Ultrasonic propagation in suspensions. A comparison of a multiple scattering and an effective medium approach," J. Acoust. Soc. Am. **85**, 535–540 (1989)], and in view the fact that validating data are scarce, the possible use of an effective medium theory is left as an open issue here.

[12] Since the PMM layer of the simple three-layer sample has significant shear properties, the actual value of the shear modulus of PMM must be used in implementing phase 3 for measurements made on this sample. However, this presents no difficulty since the shear modulus of PMM is known.

[13] As discussed in Sec. II, these rotator shaft angles ϕ must be corrected using Eq. (1) to obtain the incidence angles θ.

[14] This panel is composed of three macrovoided viscoelastic layers and a fourth layer that is a 0.95-cm ($\frac{3}{8}$-in.) steel backing plate. The first layer has 5-cm thickness, the second layer 4-cm thickness, and the third layer 3-cm thickness. The acoustical properties of the layers are unknown.

[15] The endpoints of the data windows depicted in Fig. 8 were chosen to be consistent with Eq. (4). However, the *start* points of these data windows avoid the first 300 data points permitted by Eq. (4). This is done to account for the noncausal nature of the ONION model. (See Ref. 4.) Note that the number of data points given for each of the windows in Fig. 8 corresponds to a data measured rate of 2 MHz, which differs from the 4 MHz data measurement rate used in the example given in connection with Eq. (4).